Analyst

Accepted Manuscript

This article can be cited before page numbers have been issued, to do this please use: J. Liu, J. Zeng, Y. Tian and N. Zhou, *Analyst*, 2017, DOI: 10.1039/C7AN01476G.

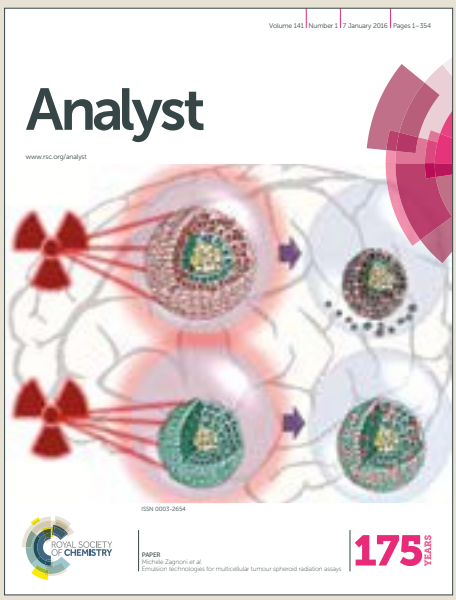

ROYAL SOCIETY OF CHEMISTRY

rsc.li/analyst

View Article Online
DOI: 10.1039/C7AN01476G

Analyst

PAPER

Aptamer and functionalized nanoparticles-based strip biosensor for on-site detection of kanamycin in food samples

Received 00th January 20xx,
Accepted 00th January 20xx

DOI: 10.1039/x0xx00000x

www.rsc.org/

Jing Liu, Jingyi Zeng, Yaping Tian and Nandi Zhou*

A lateral flow strip biosensor for fast, sensitive, low-cost and on-site detection of kanamycin was developed by using kanamycin-specific aptamer-modified gold nanoparticles (AuNPs-apt) as probe and oligonucleotide DNA1-modified silver nanoparticles (AgNPs-DNA1) as signal amplification element. Through the complementary sequences of DNA1 and the aptamer, AgNPs-DNA1-apt-AuNPs complex can be formed and further captured on the test zone of the strip, where a capture probe DNA2 complementary to 3'-terminal of DNA1 was immobilized. The presence of kanamycin can competitively bind to the aptamer, then inhibit the formation of the complex and the accumulation of AuNPs on the test zone. AuNPs-apt can finally be captured on the control zone via the specific binding between biotin and streptavidin. The assay avoids the multiple incubation and washing steps, and can be completed within 10 min. By observing the color change of the test zone, a qualitative detection for kanamycin can be achieved by naked eyes, with the visual limit of 35 nM. Meanwhile, a linear detection range of 1-30 nM with a low detection limit of 0.0778 nM for quantitative analysis can be achieved by using a scanning reader. The lateral flow strip biosensor exhibited high specificity and stability. Moreover, it was applied to detect kanamycin in various food samples, indicating its great potential in field testing.

Introduction

Antibiotics, a class of secondary metabolites, have anti-pathogen and other activities. Because antibiotics can effectively inhibit detrimental bacteria and prevent a series of infections,[1] they have been widely used in the development of modern animal husbandry. As a broad spectrum of aminoglycoside antibiotic, kanamycin has been used as human and veterinary medicine due to its inhibition of the growth of Gram-negative and Gram-positive bacteria.[2] However, the excessive use of kanamycin leads to its accumulation in animal-derived food and ultimate uptake by human,[3] which will cause serious side effects, such as ototoxicity and nephrotoxicity.[4] For consumer protection, the European Union has established maximum residue limits (MRLs) of 150 μg/kg for kanamycin in milk.[5] Nowadays, a variety of techniques have been developed for detection of antibiotic residues including kanamycin, e.g. ELISA,[6] capillary zone electrophoresis (CZE),[7] HPLC,[8] surface plasmon resonance (SPR)[9] and electrochemical analysis.[10] Although these conventional methods can detect kanamycin accurately, their application is still limited due to the requirement of specialized equipments, complicated operation, susceptible to interference, time-consuming or low sensitivity.[11,12] Therefore, it is important to establish a rapid, specific and sensitive method for on-site detection of kanamycin and other antibiotic residues.

Lateral flow test strip biosensors are promising approaches for on-site rapid detection of a variety of targets owing to their long-term stability, short assay time, low cost and no requirements for complicated equipments and skilled technicians.[13,14] The first report for strip analysis was proposed in 1956 by Plotz and Singer.[15] Since then, test strips have been widely developed and applied in the field of clinical diagnosis, environment and food monitoring.[16-18] So far, most of these strip biosensors use antibodies or specific enzymes as target-recognition elements. The use of antibodies or enzymes may encounter some issues, such as poor pH and thermo-stability, high cost, or lack of antibodies with good performance or suitable enzymes, *etc*. Aptamers (apt) generally indicate short single-stranded DNA or RNA with high affinity for the targets, which are obtained by *in vitro* screening known as SELEX.[19] Due to their high specificity, high stability, easy to modify and regenerate over antibodies,[20,21] aptamers have been widely used to fabricate biosensors for various small molecules, proteins and cells.[22-25] Since the report of kanamycin-specific aptamer,[26] it has been used as recognition element in a variety of aptamer-based kanamycin biosensors.[27-30] To explore the application of the aptamers in the fabrication of strip biosensors will provide alternative ways for fast detection of diverse targets, and may have great prospect in drug analysis,

The Key Laboratory of Carbohydrate Chemistry and Biotechnology, Ministry of Education, School of Biotechnology, Jiangnan University, Wuxi 214122, China. E-mail: zhounandi@jiangnan.edu.cn.
Electronic Supplementary Information (ESI) available: [Experimental of detection of real samples and Fig. S1-S3]. See DOI: 10.1039/x0xx00000x

View Article Online
DOI: 10.1039/C7AN01476G

disease prevention and targeted therapy.[31-34] Actually, aptamer-based strips have already exhibited excellent characteristics, such as wide detection spectrum, high stability and low-cost.[35,36] Compared with those antibody-based strips, the test strips based on aptamers have equivalent or even higher sensitivity.[37] Such test strips have been applied in the detection of nucleic acids,[38,39] toxins,[37,40] ions,[41,42] small molecular compounds,[43,44] proteins,[45] and microbials.[46] However, to the best of our knowledge, aptamer-based strip biosensors for antibiotic residues have not been reported yet.

In this study, we developed an aptamer and functionalized nanoparticles-based dry-reagent strip biosensor for potential on-site detection of kanamycin. In the strip biosensor, gold nanoparticles (AuNPs) were used as color probe, and silver nanoparticles (AgNPs) were used as signal amplification element. The strip can be used to detect kanamycin in various food samples either qualitatively by naked eyes or quantitatively by a scanning reader.

Experimental

Materials and reagents

Kanamycin, streptavidin, tris-(2-carboxyethyl)-phosphine hydrochloride (TCEP) and dATP were purchased from Sangon Biotech Co., Ltd (Shanghai, China). Silver nitrate was obtained from Sigma-Aldrich (St. Louis, MO, USA). Hydrogen tetrachloroaurate hydrate ($HAuCl_4 \cdot 4H_2O$), sodium citrate, sodium borohydride ($NaBH_4$) and sodium desoxycholate were procured from Sinopharm Chemical Reagent Co., Ltd (Shanghai, China). Sample pad, conjugate pad, nitrocellulose membrane, absorption pad and adhesive backing were purchased from Jieyi Biotechnology Co., Ltd (Shanghai, China). Other chemicals were of analytical grade. All solutions were prepared with ultrapure water (18.2 MΩ cm) obtained from a Millipore water purification system.

All the oligonucleotides including kanamycin-specific aptamer, DNA1 and DNA2 were synthetized and HPLC-purified by Sangon Biotech Co., Ltd. The specific sequences of the aptamer, DNA1 and DNA2 are listed as follows:

Aptamer: 5'-HS-$(CH_2)_6$-TGGGGGTTGAGGCTAAGCCGA-biotin-3'[26]

DNA1: 5'-HS-$(CH_2)_6$-TCAGTCGGCTTAGCCGTCCA***ACGTCAGATCC***-3'

DNA2: 5'-biotin-CCGAT***GGATCTGACGT***-3'

Underlined and italic letters represent the complementary sequences.

Synthesis and modification of gold nanoparticles (AuNPs) and silver nanoparticles (AgNPs)

The preparation of AuNPs is according to the procedure reported previously.[47] 100 mL of 0.01% (w/v) $HAuCl_4$ was put into a 250 mL round bottom flask, stirred and heated. After boiling for 2 min, 3.5 mL of 1% (w/v) sodium citrate was added rapidly with stirring. The mixture was continuously stirred and heated for 15 min, and then stirred at room temperature for another 30 min. The as-prepared AuNPs were concentrated 5 times by heating and evaporating the excessive water until a final volume of 20 mL was reached. After cooling to room temperature, the prepared AuNPs solution was stored at 4°C in the dark.

The preparation of AgNPs is according to the reported method,[48] using silver nitrate as raw material, sodium borohydride as reducing agent and sodium deoxycholate as stabilizer and chiral inducer. Firstly, 100 mL of 1 mM $AgNO_3$ and 100 mL of 2 mM sodium deoxycholate were mixed and aged at pH 7.0 for 24 h. Then freshly prepared 0.858 mL of 20 mM $NaBH_4$ was added dropwise in ice bath with vigorous stirring. After 10 min reaction, AgNPs were prepared and then stored at 4°C in the dark.

After the preparation of the previous nanoparticles, oligonucleotides were covalently immobilized on the surface of the nanoparticles via metal-S bonds. The preparation of the aptamer-modified AuNPs (AuNPs-apt) and DNA1-modified AgNPs (AgNPs-DNA1) is referring to the reported procedures.[49] Briefly, 15 μL of 1 mM TCEP was mixed with 30 μL of 100 μM aptamer or DNA1 to activate thiol group of aptamer/DNA1. Then the mixture was added into 1 mL of the prepared AuNPs/AgNPs and stirred at room temperature for 1 h. After that, 30 μL of 15 mM dATP was added to the solution and stirred for 35 min, followed by the addition of 20 μL of 1 M NaCl and incubation at room temperature for 30 min and then at 4°C for 6 h to increase the stability of the modified nanoparticles. Finally, the unbound oligonucleotides were removed by centrifugation at 8000 r/min for 20 min at 4°C. And the pellet was re-suspended in 1 mL of 20 mM Na_3PO_4 containing 0.5% Tween-20, 5% BSA, 10% sucrose and 0.5% Triton X-100. The modified nanoparticles were stored at 4°C in the dark.

Preparation of streptavidin-biotin-DNA2 conjugate

DNA2 was designed as capture probe to capture AgNPs-DNA1-apt-AuNPs complex on the test zone. To immobilize DNA2 on the test zone, streptavidin-biotin-DNA2 conjugate was prepared using biotinylated DNA2 and streptavidin via the high affinity between streptavidin and biotin. Streptavidin was dissolved in 10 mM PBS (pH 7.4) to the concentration of 1 mg/mL. Then 5 μL streptavidin and 20 μL of 10 μM DNA2 were mixed and incubated at 4°C for 2 h to allow the complete binding between streptavidin and biotinylated DNA2. After that, the prepared streptavidin-biotin-DNA2 conjugate was further incubated with 10 μL of 5 mM biotin to completely block the remaining binding sites of streptavidin. The excessive DNA2 and biotin was removed by centrifugation with ultrafiltration tube (30 kDa). The prepared streptavidin-biotin-DNA2 was stored at 4°C.

Assembly of the lateral flow strip biosensor

The strip biosensor consists of sample pad, conjugate pad, nitrocellulose membrane (NC membrane), absorption pad and PVC adhesive backing.

After cutting into the appropriate size, the conjugate pad and the sample pad were immersed in the treatment solution (0.1 M Tris-HCl buffer containing 1% NaCl, 0.5% Tween-20, 1%

View Article Online
DOI: 10.1039/C7AN01476G

BSA, 2% sucrose and 1% TritonX-100, pH 8.2) for 30 min, and then dried at 45°C. Then 10 µL of 5 µM AuNPs-apt and 10 µL of 2 µM AgNPs-DNA1 (the concentrations refer to DNA on the functionalized nanoparticles) were spread evenly on the conjugate pad, which was then dried in a thermostatic chamber at 37°C for 2 h.

To prepare the strip biosensor, NC membrane and the pads were overlapped and pasted on the adhesive backing (Scheme 1). Then 1 µL streptavidin-biotin-DNA2 conjugate was used to draw a line on the NC membrane near the conjugate pad to construct the test zone (T zone). And 1 µL of 0.5 mg/mL streptavidin was used to draw a line on the NC film near the absorption pad to construct the control zone (C zone). The distance between T zone and C zone was fixed to 5 mm. After drawing the T and C zones on NC membrane, the strips were dried at 37°C for 1 h. Finally, the assembled strip biosensors were stored in tin foil bags at 4°C.

Detection of kanamycin using the strip biosensor

Kanamycin was diluted with saline sodium citrate (SSC) containing 1% BSA (pH 7.0) to different concentration as the test solution. The test strips were placed in the cartridges. 100 µL of the test solution was added into the sample wells on the sample pad. Due to the siphon action of the capillary, the test solution will migrate through the whole strip from the sample pad to the absorption pad. This procedure can be completed within 10 min. Red bands can be observed on the T zone and C zone, due to the accumulation of AuNPs. Thus the evaluation can be achieved visually. For quantitative analysis of kanamycin, the optical density (expressed in peak area) of the T zone was determined using a scanning reader (Jieyi Biotechnology Co., Ltd, Shanghai, China).

Detection of kanamycin in real food samples

To verify the performance of the strip biosensor for real food samples, kanamycin was added into honey, milk and milk powder to prepare artificially kanamycin-contaminated samples. For honey samples, the artificially contaminated honey was directly diluted 10 folds with SSC. (Milk and milk powder samples see in the supplementary information). The detection was then carried out with the test strips as described above.

Results and discussion

Principle of the strip biosensor for kanamycin

The configuration and principle of detection of the aptamer and functionalized nanoparticles-based lateral flow strip biosensor are shown in Scheme 1. AuNPs-apt and AgNPs-DNA1 have already been modified on the conjugate pad before the assembly of the strip. Streptavidin-biotin-DNA2 conjugate and free streptavidin were immobilized on the T zone and C zone of NC membrane respectively. Since DNA1 is complementary to the aptamer at its 5'-terminal and complementary to DNA2 at its 3'-terminal, AgNPs-DNA1-apt-AuNPs complex can be formed and further captured on the test zone of the strip

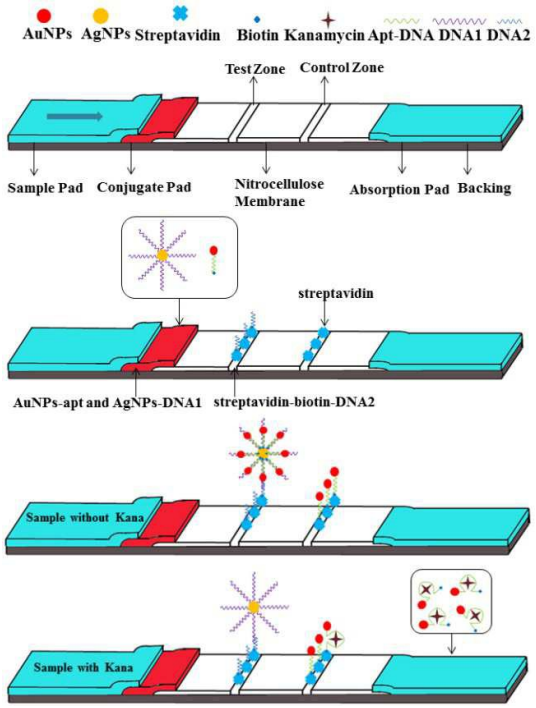

Scheme.1 Schematic diagram of configuration and detecting principle of the strip biosensor.

through the hybridization between these complementary oligonucleotides in the absence of kanamycin. Thus a clear deep red band can be observed on the T zone due to the accumulation of AuNPs. The excessive AuNPs-apt will further migrate to the C zone on the strip and be captured through the binding of biotin at the 3'-end of the aptamer and streptavidin immobilized on the C zone. Therefore a red band can also be observed on the C zone. In the presence of kanamycin, it binds specifically to the aptamer modified on AuNPs, dehybridizes the duplex between the aptamer and DNA1, and then releases AuNPs-apt from AgNPs-DNA1-apt-AuNPs complex. The released AuNPs-apt can be captured on the C zone through biotin-streptavidin interaction. Due to the reduced accumulation of AuNPs, light red color will appear on the T zone. The shade of the color on the T zone is negatively correlated to the concentration of kanamycin. Therefore, a strip exhibiting two red bands represents a negative result, whereas a strip exhibiting a lighter or completely faded T zone represents a positive result.

Synthesis and modification of AuNPs and AgNPs

The prepared AuNPs and AgNPs were characterized by transmission electron microscopy (TEM) and UV-vis spectrophotometer. As shown in Fig. 1a and Fig. 1b, the prepared AuNPs and AgNPs were well dispersed and had uniform particle sizes of 13 nm and 20 nm, respectively. The typical adsorption peaks of AuNPs and AgNPs at 520 nm and 420 nm respectively can be also observed in UV-vis spectra (Fig. S1).

View Article Online
DOI: 10.1039/C7AN01476G

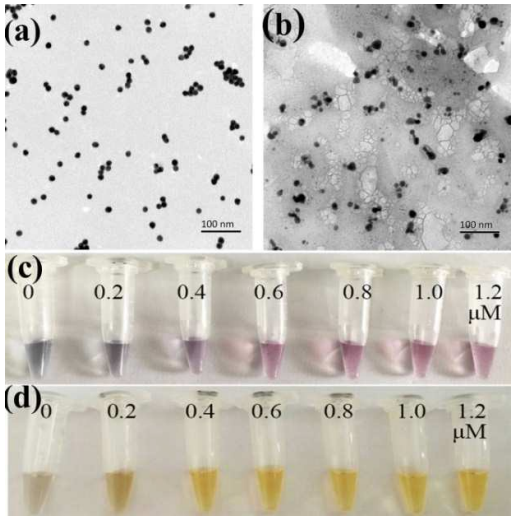

Fig. 1 (a) TEM image of AuNPs; (b) TEM image of AgNPs; (c) Incubation of AuNPs modified with different concentration of the aptamer in NaCl; (d) Incubation of AgNPs modified with different concentration of DNA1 in NaCl.

The nanoparticles were then functionalized with oligonucleotides to obtain AuNPs-apt and AgNPs-DNA1. The concentration of the aptamer or DNA1 used to modify the nanoparticles can influence the coverage of these oligonucleotides on the surface of the nanoparticles and the performance of the strip sensor. The modified oligonucleotides are not only responsible for recognition of the target kanamycin or the complementary sequence, but also for maintaining the stability of the nanoparticles. It is well-known that bare AuNPs or AgNPs aggregate and change their color in high concentration of NaCl, and the modification of nucleic acids on the surface of these nanoparticles can greatly improve their stability and maintain their dispersity.[50] Therefore, the stability of the modified nanoparticles in NaCl solution was chosen as an index to optimize the concentration of the oligonucleotides during the functionalization of the nanoparticles. The prepared AuNPs were incubated with different concentration of the aptamer, and then NaCl was added into the solution to a final concentration of 20 mM. As shown in Fig. 1c, when the concentration of the aptamer was lower than 0.6 μM, the color of AuNPs-apt turned to grey after the addition of NaCl, indicating the aggregation of AuNPs. Therefore, 0.6 μM aptamer was chosen to modify AuNPs. Similarly, the prepared AgNPs were incubated with different concentration of DNA1, and then NaCl was introduced. As shown in Fig. 1d, after incubation with DNA1 with the concentration higher than 0.4 μM, the obtained AgNPs-DNA1 maintained stable in NaCl solution. Thus 0.4 μM DNA1 was chosen to modify AgNPs.

Optimization of the parameters

In order to achieve high sensitivity and signal-to-noise ratio, low detection limit and high stability, the parameters for strip preparation, including the concentration of streptavidin, streptavidin-biotin-DNA2 conjugate and NaCl, the amount of AuNPs-apt and AgNPs-DNA1, the type of NC membrane and running buffer on conjugate pad were optimized. The conditions used in the preparation of the strip can ensure the appearance of clear deep red bands on the T and C zones.

Streptavidin immobilized on the C zone is responsible for the capturing of excessive AuNPs-apt that cannot form AgNPs-DNA1-apt-AuNPs complex and be captured on the T zone, or AuNPs-apt released from the complex due to the binding of kanamycin to the aptamer. Streptavidin solution with different concentration was immobilized on the C zone, then SSC buffer was applied on the strip, and the color density of the C zone was determined by the colloidal gold scanning reader. As shown in Fig. 2a, the optical density of the C zone, expressed in peak area, increases with the concentration of streptavidin. When the concentration of streptavidin is higher than 0.5 mg/mL, the peak area almost maintains constant. Thus, 0.5 mg/mL streptavidin solution was chosen to construct the C zone.

Streptavidin-biotin-DNA2 conjugate was immobilized the T zone to capture AgNPs-DNA1-apt-AuNPs complex through the hybridization between the complementary sequence of DNA1 and DNA2. Thus the coverage of streptavidin-biotin-DNA2 on the T zone is a critical factor to ensure the efficient capture of the complex and the optical density of the T zone. Different concentration of streptavidin-biotin-DNA2 conjugate ranging from 0.001 to 100 μM (refer to the concentration of DNA2) was used to construct the T zone, whereas other conditions remained consistent. The results are shown in Fig. 2b. With the increase of the concentration of the conjugate, the peak area of the T zone increases, and the color density almost remains stable when the concentration reaches 20 μM. Therefore, 20 μM streptavidin-biotin-DNA2 conjugate was chosen to construct the T zone.

The concentration of NaCl used during the preparation of the T and C zones has great influence on the color shown on the zones after detection. Generally, on the one hand, if the concentration of salt is too high, the appeared color on the strip is too dark. On the other hand, if the concentration of salt is too low, the strip cannot show a clear band due to the hydrophilicity of NC membrane.[51] Streptavidin-biotin-DNA2 conjugate and streptavidin were respectively prepared with different concentration of NaCl in the range of 0-2 M, whereas other experimental conditions remained unchanged. The relationship between the peak area of the T zone and the concentration of NaCl is shown in Fig. 2c. When the concentration of NaCl is lower than 0.5 M, the color band on the strip is divergent, and the peak area is reduced. As the concentration is higher than 0.5 M, obvious bands appear on the strip, and the increase of the peak area levels off. Thus, 0.5 M was chosen as the optimal concentration of NaCl to prepare streptavidin-biotin-DNA2 conjugate and streptavidin.

View Article Online
DOI: 10.1039/C7AN01476G

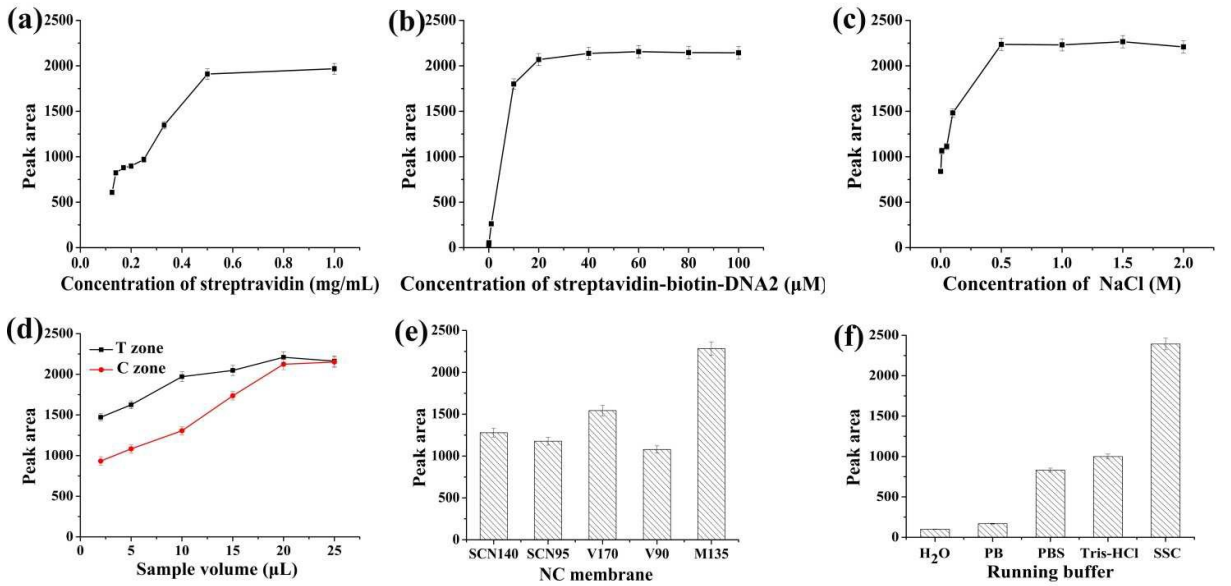

Fig. 2 Optimization of parameters: (a) concentration of streptavidin; (b) concentration of streptavidin-biotin-DNA2 conjugate; (c) concentration of NaCl; (d) the amount of AuNPs-apt and AgNPs-DNA1 added on the conjugate pad; (e) the type of NC membrane; (f) the type of running buffer.

The amount of AuNPs-apt and AgNPs-DNA1 applied on the conjugate pad is the key factor in the optical density of the bands on the T and C zones, and thus was investigated. Equal volumes of AuNPs-apt and AgNPs-DNA1 were firstly mixed, and then different volume of the mixture was applied on the conjugate pad. From Fig. 2d, it can be seen that the optical intensity of the T and C zones is proportional to the applied volume of the mixture of AuNPs-apt and AgNPs-DNA1, and substantially keeps constant when the volume reaches 20 μL. Thus the optimal volume of AuNPs-apt and AgNPs-DNA1 applied on the conjugate pad is 20 μL.

Different types of NC membrane were used to prepare the strips and their influence on detection was investigated. Several frequently used NC membranes, including Sartorius CN140 (SCN140), Sartorius CN95 (SCN95), Vivid 170 (V170), Vivid 90 (V90) and Millipore 135 (M135) were employed to assemble the strips, and their color intensity of the T zone under the same experimental conditions was determined (Fig. 2e). Among them, Millipore 135 membrane showed the best performance and was chosen to fabricate the strip biosensor.

The running buffer used in detection has huge impact on the sensitivity and specificity, therefore was also optimized. Five different running buffers (H_2O; 10 mM phosphate buffer, pH 7.0; 10 mM phosphate buffer saline, pH 7.0; 10 mM Tris-HCl, pH 7.0; and 15×SSC (0.225 M sodium citrate containing 2.25 M NaCl, pH 7.0) containing 1% BSA were selected as candidates. As shown in Fig. 2f, the most suitable running buffer is SSC containing 1% BSA.

The performance of the strip biosensor

After the optimization of the above experimental parameters, the strip biosensor was fabricated under the optimal conditions and used to detect kanamycin qualitatively by naked eyes or quantitatively by using a scanning reader.

The sensitivity and detection limit of the strip biosensor were evaluated by using a series of kanamycin standard solution within the concentration range of 0-400 nM. As shown in Fig. 3a, in the absence of kanamycin, clear red color can be observed on both the T zone and the C zone. With the increase of the concentration of kanamycin, the color density of the C zone is basically unchanged, whereas the red band on the T zone is gradually shallow. As the concentration of kanamycin reaches 35 nM, the T zone is completely faded. Therefore, the visual detection limit of the strip sensor is estimated to be 35 nM. Furthermore, after the determination of the optical density of the T zone, the relationship between the peak area of the T zone and the concentration of

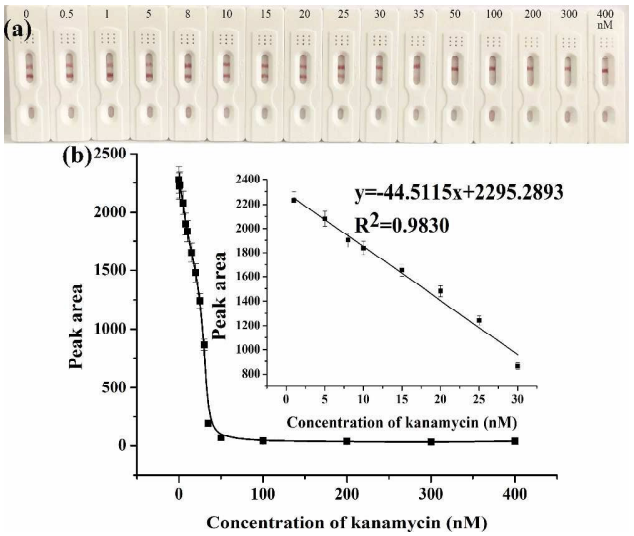

Fig. 3 (a) The photograph of the strips applied with different concentrations of kanamycin; (b) Calibration curve corresponding to the peak area of the T zone and the concentration of kanamycin in standard solution; Inset shows the derived linear relationship.

View Article Online
DOI: 10.1039/C7AN01476G

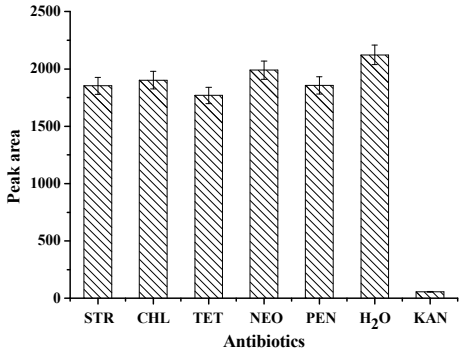

Fig. 4 Specificity evaluation of the strip biosensor.

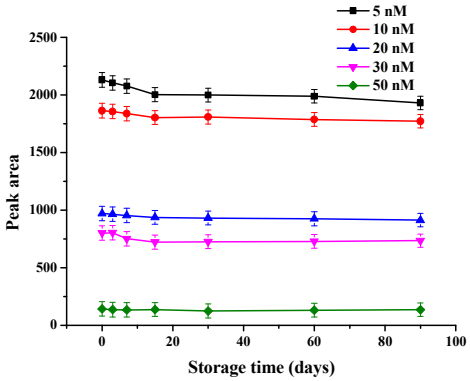

Fig. 5 Storage stability of the strip biosensor.

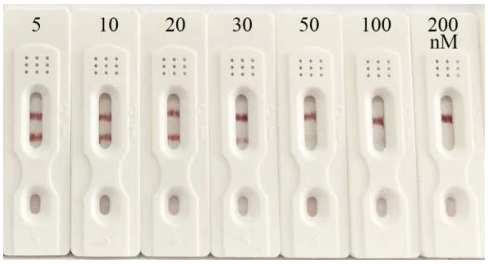

Fig. 6 Detection of kanamycin in honey samples.

kanamycin was plotted and shown in Fig. 3b. The peak area is gradually decreased with the increased concentration of kanamycin, and no longer changed when the concentration of kanamycin is higher than 50 nM. This is in accordance with the observation. Within the concentration range of 1-30 nM, a linear relationship can be derived between the peak area and the concentration of kanamycin, with the linear regression equation of $y=-44.5115x+2295.2893$, $R^2=0.9830$, where x represents the concentration of kanamycin (nM), and y represents the peak area of T zone. The detection limit was estimated to be 0.0778 nM (S/N=3), which indicates high sensitivity of the strip biosensor.

To verify the accuracy of the strip biosensor, the widely recognized method in antibiotics detection, HPLC was carried out simultaneously. Different concentrations of kanamycin solution (3, 10 and 15 mM) were prepared and analyzed by HPLC and the aptamer-based strip biosensor, respectively. The results are shown in Table 1. Both methods exhibit excellent accuracy. Although the RSD value of the strip is higher than that of HPLC, it is still good enough for generally applications. Moreover, the sensitivity of the test strip is much higher than that of the HPLC method.

To evaluate the specificity of the prepared strip biosensor, it was challenged by a series of other antibiotics, including streptomycin (STR), chloramphenicol (CHL), tetracycline (TET), neomycin (NEO), penicillin (PEN) and water. The concentration of the antibiotics was fixed as 100 nM. All the detection conditions were the same, and the optical density of the T zone was determined and compared, as shown in Fig. 4. Significant fade on the T zone only appears in the presence of kanamycin. For other antibiotics, the peak area of the T zone shows only slight decrease as compared to that of the control (water). Therefore, the strip biosensor is highly specific for kanamycin.

The stability of the strip biosensor was also checked. The strips were stored at 4°C under dry condition. They were used to detect different concentration of kanamycin (5, 10, 20, 30 and 50 nM) after 3, 7, 15, 30, 60 and 90 days' storage. The results are shown in Fig. 5. No significant change in the peak area occurs after storage for 3 months (the decrease of the peak area was within 0.73-8.37%), indicating satisfactory stability of the strip biosensor.

Detection of kanamycin in real samples

To evaluate the practicability of the prepared strip biosensor, artificially contaminated food samples, including honey, milk and milk powder were analyzed by using the strips. Different concentration of kanamycin (5, 10, 20, 30, 50, 100 and 200 nM) was introduced into kanamycin-free honey, and the honey samples were detected directly after dilution for 10 folds with SSC. Then the samples were applied to the strips, and the results are shown in Fig. 6 (the results of milk and milk powder samples were shown in Fig. S2 and Fig. S3). The visual detection limits for kanamycin in honey, milk and milk powder samples were estimated to be 50 nM, 100 nM and 200 nM, respectively. Thus the prepared strip biosensor can be used for

Table 1 The comparison of the strip biosensor with HPLC assay. Average value and RSD were from three independent experiments.

	Test strip biosensor		HPLC	
Concentration of kanamycin (mM)	Average detection value (mM)	RSD (%)	Average detection value (mM)	RSD (%)
3	3.09	2.08	2.95	0.59
10	10.12	4.41	10.05	0.25
15	14.91	3.78	15.03	0.32

View Article Online
DOI: 10.1039/C7AN01476G

detecting actual food samples. And the detection limits are basically equivalent to those of antibody-based strip for kanamycin.[52] However, different matrices of the food samples do influence the sensitivity of detection at a certain extent. For example, the matrix of milk and milk powder can interfere in the detection, and the pretreatment can lead to slight loss of the target. Thus the visual detection limits for milk and milk powder samples are higher than that of the standard solution. Nevertheless, the matrix of honey has negligible effect on the detection. No pretreatment is required before detection, and the detection limit is even similar to that of the standard solution.

Conclusions

In summary, a lateral flow strip biosensor for kanamycin was successfully developed by employing the aptamer-based molecular recognition and nanoparticles-based coloration and signal-amplification. After optimization of key parameters, the strip exhibits excellent sensitivity, as well as high specificity and high stability. The operation of the detection is simple and can be completed in 10 min. Moreover, the strip biosensor can be applied to detect kanamycin in different food samples. Thus it may have great prospect in application scenarios where on-site detection is required.

Acknowledgements

The authors thank the National Natural Science Foundation of China (no. 31271860) and the Fundamental Research Funds for the Central Universities (JUSRP51402A) for financial support of this work.

References

1 A. Kling, C. Chatelle, L. Armbrecht, E. Qelibari, J. Kieninger, C. Dincer, W. Weber and G. Urban, *Anal. Chem.*, 2016, **88**, 10036-10043.
2 Q. G. Liao, B. H. Wei and L. G. Luo, *Microchim. Acta*, 2016, **184**, 627-632.
3 R. Y. Robati, A. Arab, M. Ramezani, F. A. Langroodi, K. Abnous and S. M. Taghdisi, *Biosens.Bioelectron*., 2016, **82**, 162-172.
4 R. Z. Li, Y. Liu, L. Cheng, C. Z. Yang and J. D. Zhang, *Anal. Chem.*, 2014, **86**, 9372-9375.
5 Q. G. Liao, B. H. Wei and L. G. Luo, *Microchim. Acta*, 2017, **184**, 627–632.
6 C. Li, Y. Y. Zhang, S. A. Eremin, O. Yakup, G. Yao and X. Y. Zhang, *Food Chem*., 2017, **227**, 48-54.
7 C. Z. Yu, Y. Z. He, G. N. Fu, H. Y. Xie and W. E. Gan, *J. Chromatogr. B,* 2009, **877**, 333-338.
8 C. Sheu, S. C. Chen and C. C. Lo, *J. Environ. Sci. Heal. B,* 2010, **45**, 478-484.
9 F. Fernandez, D. G. Pinacho, F. Sanchez-Baeza and M. P. Marco, *J. Agric. Food Chem*., 2011, **59**, 5036-5043.
10 R. Liu, Z. H. Yang, Q. Guo, J. C. Zhao, J. Ma, Q. Kang, Y. F. Tang, Y. Xue, X. H. Lou and M. He, *Electrochim. Acta*, 2015, **182**, 516-523.
11 Y. Zhu, P. Chandra, K. M. Song, C. Ban and Y. B. Shim, *Biosens. Bioelectron*., 2012, **36**, 29-34.
12 H. Z. Wang, Y. Wang, S. Liu, J. H. Yu, Y. N. Guo, Y. Xu and J. D. Huang, *Biosens. Bioelectron*., 2016, **80**, 471-476.
13 L. M. Hu, K. Luo, J. Xia, G. M. Xu, C. H. Wu, J. J. Han, G. G. Zhang, M. Liu and W. H. Lai, *Biosens. Bioelectron*., 2017, **91**, 95-103.
14 B. H. Park, S. J. Oh, J. H. Jung, G. Choi, J. H. Seo, D. H. Kim, E. Y. Lee and T. S. Seo, *Biosens. Bioelectron*., 2017, **91**, 334-340.
15 C. M. Plotz and J. M. Singer, *Am. J. Med.*, 1956, **21**, 888-892.
16 W. J. Liu, M. F. Zhang, X. Y. Liu, A. Sharma and X. T. Ding, *Biosens. Bioelectron.*, 2017, **96**, 213-219.
17 Q. Zhang, Q. Y. Qu, S. S. Chen, X. W. Liu and P. W. Li, *Food Chem.*, 2017, **231**, 295-300.
18 Z. P. Liang, W. Z. Ha, Z. L. Xiao, H. T. Lei, Y. D. Shen, Y. M. Sun, H. Wang, J. Y. Yang and Z. L. Xu, *Food Anal. Method*., 2017, **10**, 2444-2453.
19 T. Kunii, S. Ogura, M. Mie and E. Kobatake, *Analyst*, 2011, **136**, 1310-1312.
20 K. H. Leung, H. Z. He, D. S. H. Chan, W. C. Fu, C. H. Leung and D. L. Ma, *Sensor. Actuat. B: Chem.*, 2013, **177**, 487-492.
21 X. Sun, F. L. Li, G. H. Shen, J. D. Huang and X. Y. Wang, *Analyst*, 2014, **139**, 299-308.
22 S. Cheng, B. Zheng, M. Z. Wang, M. H. W. Lam and X. W. Ge, *Talanta*, 2013, **115**, 506-511.
23 W. H. Zhou, P. J.Huang, J. Ding and J. W. Liu, *Analyst*, 2014, **139**, 2627-2640.
24 Y. Y. Xu, T.Han, X. Q. Li, L. H. Sun, Y. J. Zhang and Y. S. Zhang, *Anal. Chim. Acta*, 2015, **891**, 298-303.
25 J. J. Li, M. Xu, H. P. Huang, J. J. Zhou, E. S. Abdel-Halimb, J. R. Zhang and J. J. Zhu, *Talanta*, 2011, **85**, 2113-2120.
26 K. M. Song, M.Cho, H.Jo, K. Min, S. H. Jeon, T. Kim, M. S. Han, J. K. Ku and C. Ban, *Anal. Biochem*., 2011, **415**, 175-181.
27 C. S. Wang, C. Liu, J. B. Luo, Y. P. Tian and N. D. Zhou, *Anal. Chim. Acta*, 2016, **936**, 75-82.
28 M. Chen, N. Gan, Y. Zhou, T. H. Li, Q. Xu, Y. T. Cao and Y. J. Chen, *Sensor. Actuat. B: Chem.*, 2017, **242**, 1201-1209.
29 Y. Y. Xu, T. Han, X. Q. Li, L. H. Sun, Y. J. Zhang and Y. S. Zhang, *Anal. Chim. Acta*, 2015, **891**, 298-303.
30 Y. Y. Xu, L. H. Sun, X C. Huang, Y. Y. Sun and C. H. Lu, *Anal. Methods*, 2016, **8**, 726-730.
31 N. Cheng, Y. C. Xu, Y. B. Luo, L. Y. Zhu, Y. T. Zhang, K. L. Huang and W. T. Xu, *Chem. Commun*., 2017, **53**, 4222-4225.
32 G. D. Liu, X. Mao, J. A. Phillips, H. Xu, W. H. Tan and L. W. Zeng, *Anal. Chem.*, 2009, **81**, 10013-10018.
33 M. Jauset-Rubio, M. Svobodova, T. Mairal, C. McNeil, N. Keegan, M. S. El-Shahawi, A. S. Bashammakh, A. O. Alyoubi and C. K. O'Sullivan, *Anal.Chem.*, 2016, **88**, 10701-10709.
34 J. H. Chen, Z. Y. Fang, P. C. Lie and L. W. Zeng, *Anal. Chem.*, 2012, **84**, 6321-6325.
35 G. Y. Shen, S. B. Zhang and X. Hu, *Clin. Biochem.*, 2013, **46**, 1734-1738.
36 W. B. Shim, M. J. Kim, H. Mun and M. G. Kim, *Biosens. Bioelectron*., 2014, **62**, 288-294.
37 L. B. Wang, W. W. Ma, W. Chen, L. Q. Liu, W. Ma, Y. Y. Zhu, L. G. Xu, H. Kuang and C. L. Xu, *Biosens. Bioelectron*., 2011, **26**, 3059-3062.
38 Y. Gao, X. L. Deng, W. Wen, X. H. Zhang and S. F. Wang, *Biosens. Bioelectron*., 2017, **92**, 529-535.
39 X. Mao, H. Xu, Q. X. Zeng, L. W. Zeng and G. D. Liu, *Chem. Commun.*, 2009, **21**, 3065-3067.
40 L. B. Wang, W. Chen, W. W. Ma, L. Q. Liu, W. Ma, Y. Y. Zhao, Y. Zhu, L. G. Xu, H. Kuang and C. L. Xu, *Chem. Commun*., 2011, **47**, 1574-1576.
41 L. Yao, J. Teng, M. Y. Zhu, L. Zheng, Y. H. Zhong, G. D. Liu, F. Xue and W. Chen, *Biosens. Bioelectron*., 2016, **85**, 331-336.

View Article Online
DOI: 10.1039/C7AN01476G

42 Y. L. Wang, L. M. Wang, J. J. Xue, J. B. Dong, J. Cai, X. D. Hua, M. H. Wang, C. Z. Zhang and F. Q. Liu, *PloS one*, 2017, **12**, 1-13.
43 V. C. Ozalp, D. Cam, F. J. Hernandez, L. I. Hernandez, T. Schafer and H. A. Oktem, *Analyst*, 2016, **141**, 2595-2599.
44 C. Zhu, Y. Zhao, M. M. Yan, Y. F. Huang, J. Yan, W. H. Bai and A. L. Chen, *Anal. Bioanal. Chem.*, 2016, **408**, 4151-4158.
45 X. Mao, T. E. Du, Y. Y. Wang and L. L. Meng, *Biosens. Bioelectron.*, 2015, **65**, 390-396.
46 W. Wu, S. M. Zhao, Y. P. Mao, Z. Y. Fang, X. W. Lu and L. W. Zeng, *Anal. Chim. Acta*, 2015, **861**, 62-68.
47 X. F. Gao, L. P. Xu, T. T. Wu, Y. Q. Wen, X. L. Ma and X. J. Zhang, Talanta, 2016, **146**, 648-654.
48 W. T. Liu, H. Lai, R. Huang, C. T. Zhao, Y. M. Wang, X. C. Weng and X. Zhou, *Biosens. Bioelectron.*, 2015, **68**, 736-740.
49 W. L. Zhou, W. J. Kong, X. W. Dou, M. Zhao, Z. Ouyang and M. H. Yang, *J. Chromatogr. B*, 2016, **1022**, 102-108.
50 C. Y. Qin, W. Wen, X. H. Zhang, H. S. Gu and S. F. Wang, *Analyst*, 2015, **140**, 7710-7717.
51 T. M. Nargang, M. Runck, D. Helmer and B. E. Rapp, *Eng. Life Sci.*, 2016, **16**, 525-531.
52 Y. Q. Chen, Z. Q. Wang, Z. H. Wang, S. S. Tang, Y. Zhu and X. L. Xiao. *J. Agric. Food Chem.*, 2008, **56**, 2944–2952.